



23rd International Conference on Material Forming (ESAFORM 2020)

FE-based Layer Design of Deposition-Welded Semi-finished Parts for the Production of Hybrid Bevel Gear

Bernd-Arno Behrens^a, Johanna Uhe^a, Hendrik Wester^a, Tim Matthias^a and Christoph Büdenbender^{a,*}

^a*Institut für Umformtechnik und Umformmaschinen, Leibniz Universität Hannover, An der Universität 2, 30823 Garbsen, Germany*

* Corresponding author. Tel.: +49-511-762-2329; Fax: +49-511-762-3007; E-mail address: buedenbender@ifum.uni-hannover.de

Abstract

Multi-material solutions offer numerous benefits as they, in contrary to conventional monolithic parts, represent tailor-made hybrid components with enhanced application-optimisation properties. The use of hybrid semi-finished products is the approach to apply the right material in the right place. This procedure of manufacturing components helps to reduce costs and avoids the waste of resources. Within this paper, a process route is presented, which can be used to produce a hybrid bevel gear by means of tailored forming technology. For the bevel gear, C22.8 was used as base material. The wheel body was designed with 41Cr4 and X45CrSi9-3. The semi-finished product was manufactured by means of deposition welding. The resulting geometry of the semi-finished product is a cylindrical body with two thin outer layers. This article focuses on the numerical investigation of the required layer thickness, so that on the one hand a material distribution after the forming process can be adjusted in order to guarantee the longest possible service life and on the other hand a stable forming process without cracks of the surface of the layers. Due to locally different material properties of the semi-finished product, uncommon material flow occurs. Furthermore, the deposition-welded material has different flow properties than conventional material. Therefore, a material characterisation by means of upsetting test was carried out for the 41Cr4 and X45CrSi9-3 in the deposition-welded status and was compared to conventional material. The initial thickness of the deposition-welded layers was designed with the aid of numerical simulation. The initial geometry of the layers was designed in such a way that the tooth body is completely filled after forming with an optimal use of material.

© 2020 The Authors. Published by Elsevier Ltd.

This is an open access article under the CC BY-NC-ND license (<https://creativecommons.org/licenses/by-nc-nd/4.0/>)
Peer-review under responsibility of the scientific committee of the 23rd International Conference on Material Forming.

Keywords: Numerical material flow investigation; material characterisation; tailored forming

1. Introduction

The environmental friendly handling of resources is more of a topic than ever at the time. To avoid waste in the use of modern forging products it is necessary to have components, which have high durability and are manufactured in an efficient process. The focus of the automotive industry is the reduction of component weight, to save fuel consumption of modern cars with combustion engines and to compensate the high weight of batteries in electric vehicles. In addition, the cost-optimised use of materials is becoming more important. Thus, cheaper materials in areas where lower loads occur substitute high-

priced materials. Due to increasingly demanding requirements, conventional mono-material components are closer to their material-specific limits [1]. Hybrid components open up the possibility to design application-optimised parts with a high lightweight potential combining individual benefits of each material in one component. The manufacturing of multi-material by bulk metal forming represents a promising method to produce near-net-shape or ready-to-install functional components with complex geometries and outstanding mechanical properties within just a few processing steps [2]. There are several possibilities to produce hybrids parts. In recent investigations, compound forging has been often used for production of hybrid components. Besides the near-net-

2351-9789 © 2020 The Authors. Published by Elsevier Ltd.

This is an open access article under the CC BY-NC-ND license (<https://creativecommons.org/licenses/by-nc-nd/4.0/>)
Peer-review under responsibility of the scientific committee of the 23rd International Conference on Material Forming.
10.1016/j.promfg.2020.04.235

shape of hybrid components, this technology provides also a possibility to join the semi-finished products from different materials during the forging process. Examples of composite forged parts are drive flanges [3], connecting rods [4], or hybrid toothed elements [5]. Hybrid components of sheet metal and bulk metal can also be produced by compound forging [6]. The blank parts can be joined before the forming process for example by brazing, friction welding or extrusion [7]. The forming of pre-joined semi-finished products consisting of hybrid material combinations is the focus of just a few research works for bulk metal forming process. In this context, a new Collaborative Research Centre (CRC) 1153 “Tailored Forming” has been started at the Leibniz Universität Hannover to investigate innovative process chains for the manufacturing of high-performance hybrid components. In contrast to conventional production processes of hybrid bulk metal components, where the joining process takes place during the forming or at the end of the production chain, tailor-made semi-finished products are joined prior to the forming process. The Tailored Forming Technology offers a promising method for manufacturing of high-performance components with locally specific characteristics adapted to the particular application area. In [8,9], Behrens et al. present challenges arising due to different material properties and offer possible solutions for heating and forming strategies.

Within this article, the complex process chain for the production of a hybrid bevel gear is presented. The following process steps for the production of hybrid bevel gear based on the Tailored Forming Technology are required (cf. Fig. 1). At first, the different layers are applied on the cylindrical semi-finished product by means of deposition welding. This is one of the most frequently used process in joining technology since it is preferred for the use of expensive functional materials on low-priced base materials [10]. Within a subsequent hot forging process, the semi-finished product is formed to a hybrid component with a complex gear geometry. Additional processing steps such as heat treatment and machining finalise the process chain.

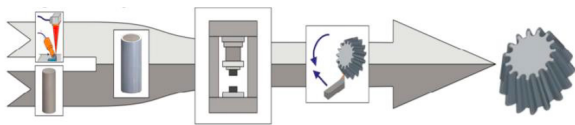


Fig. 1. Process-chain of the Tailored Forming Technology for a hybrid bevel gear

This study focuses on the numerical investigation of material flow investigation in the forging process of a hybrid bevel gear made by a cylindrical semi-finished product and two deposition welded steel layers. The aim of this numerical study is to investigate the material distribution of the thin outer layers after the forming process. The core of the semi-finished product used is made of low-cost, heat-resistant, unalloyed structural steel C22.8. The first layer is made of the martensitic steel X45CrSi9-3, which is welded onto the cylindrical core. In further research projects, a material with a defined coefficient of thermal expansion will replace this layer material. With this structure of the semi-finished product, specific residual stresses should be introduced into the bevel due to thermal tensions.

These residual stresses should act against the loads that occur during the operating process to significantly increase the service life. Finally, 41Cr4 is applied to the first layer also by deposition welding. The circumferential outer area of the gear teeth is exposed to high stresses and abrasive wear and therefore consists of a high strength material (41Cr4). Meanwhile, the inner section can consist of a low-priced steel (C22.8) in order to reduce material costs. The intermediate layer is made of high-alloy steel X45CrSi9-3.

In addition to a numerical study a material characterisation was carried out to investigate the flow behaviour of deposition welded material. This flow behaviour was compared to the flow behaviour of conventional industrial rod material. For this purpose, upsetting tests were carried out at process-related forming temperatures and strain rates. The results of the material characterisation were implemented in the simulation model. Finally, the material distribution after the forging process of hybrid bevel gear with two layers was investigated numerically depending on the initial layer thickness. The results of this numerical investigation can be used in further experimental tests to optimise the use of material of the inner and outer layers of the semi-finished product.

2. Material Characterisation

Uniaxial compression tests were carried out to determine flow curves of the investigated materials 41Cr4 and X45CrSi9-3. In this paper, the flow behavior of two specimens extracted from deposition material and conventional material was investigated. At first, cylindrical samples were taken from a welding track by wire eroding. The welding track was welded on a base material C22.8. The specimens for the second variant of sample preparation were taken from conventional rod material. The rod has a diameter of 40 mm. Fig. 2 (a) shows the baseplate and the welding track from the first preparation method and in Fig. 2 (b) the rod as well as the used specimen within this study are depicted.

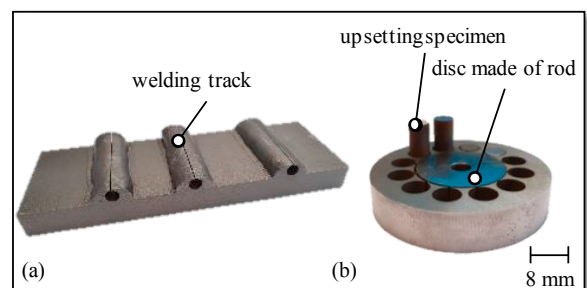


Fig. 2. (a) Base plate with welding tracks, (b) disc made of a rod with the used upsetting specimen

The specimens had a diameter of 5 mm and a height of 8 mm. The upsetting tests were carried out with the forming and quenching dilatometer DIL 850A/D+T from TA instruments. For the tests three different temperatures (900 °C, 1050 °C, 1200 °C) and three different strain rates (0.1 s⁻¹, 1 s⁻¹ and 10 s⁻¹) were investigated. The specimens were inductively heated. The samples were upset to a plastic strain of $\varphi = 0.7$.

Up to this point, the influence of friction on the measurement result is negligibly small [11,12]. The resulting force-displacement data from the testing machine was used to compute the coefficients for the analytical flow curve approach called Hensel-Spittel-10, which is described in the following equation (1):

$$\sigma_f = A \cdot e^{m_1 \cdot T} \cdot T^{m_8} \cdot \varphi^{m_2} \cdot e^{\left(\frac{m_4}{\varphi} + m_6 \cdot \varphi\right)} \cdot (1 + \varphi)^{(m_5 \cdot T)} \cdot \varphi^{(m_3 + m_7 \cdot T)} \quad (1)$$

The resulting flow stress is represented by σ_f . To compute the coefficients A, m_1 , m_2 , m_3 , m_4 , m_5 , m_6 , m_7 , m_8 , the GRG-nonlinear optimisation algorithm was used [13]. The resulting stress-strain curves for tested temperatures as well as strain rates and the resulting coefficients for the flow curve approach are discussed in chapter 4.1.

3. Numerical investigation of the bevel gear

In this study, a single-stage tool is used consisting of an upper die and a lower die. The semi-finished product is positioned between the upper and lower die. A sectional view of the used numerical model is depicted in Fig. 3 (a). The semi-finished product is divided into three parts. The core of the semi-finished product is modelled as a cylindrical deformable body and is extended by two layers which are also modelled as a deformable body (cf. Fig. 3 (b)). This numerical investigation serves to determine the thickness of the layers with the aim of an optimal material distribution in tooth body of the final hybrid bevel gear. X45CrSi9-3 is used for the first layer and 41Cr4 for the second layer. Within this numerical investigation, the flow curves of the deposition material are implemented with the analytical flow stress approach Hensel-Spittel-10. For the core material C22.8, data from the simufact database were used. Due to technical restrictions of the material and the welding process of the first layer is limited to a minimal initial thickness of 1 mm and the second layer to 1.5 mm. Finally, the semi-finished product is restricted to diameter of 30 mm and a height of 79.2 mm so that a stable forming process can be guaranteed [14]. The possible combinations of dimensions for layer thicknesses, which were investigated numerically, are presented in table 1.

Table 1. Investigated dimension of the initial outer and inner layer thickness and resulting core diameter

	A	B	C	D
Thickness outer layer in mm	1	2	1	2
Thickness inner layer in mm	1.5	1.5	3	3
Core diameter in mm	25	23	22	20

A numerical model was created with the FEM software tool simufact.forming version 16.0. To reduce the processing time of the simulation, a thirtieth model was created. This model dimension illustrates the forging process of half a tooth and is sufficient to investigate the material flow of the process. The tools were modelled as rigid bodies. The resulting coefficients for the flow curve approach Hensel-Spittel-10, which were computed with the deposition-welded material, was implemented in the numerical model. A combined friction

model was used with $m = 0.3$ and $\mu = 0.08$. The three deformable bodies were meshed with tetrahedral elements. The contact between the deformable bodies was implemented with an adhesive connection. This modelling is a numerically efficient method to determine the weld joint between the core and the two layers. The initial forging temperature was 1200 °C. Several initial layer thickness dimensions were investigated and the resulting material distribution after the forming process will be discussed in chapter 4.2.

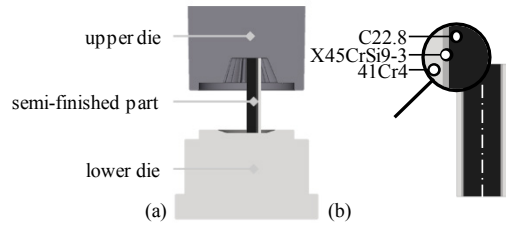


Fig. 3. (a) Tool structure for manufacturing of a hybrid bevel gear, (b) structure of the semi-finished product

4. Results

4.1. Material characterisation

The results of the material characterisation are presented in this chapter. First, the results of the determined flow behaviour of the material 41Cr4 are discussed. The resulting flow curves at the tested temperatures of 900 °C, 1050 °C and 1200 °C at strain rates 0.1 s⁻¹ are presented in Fig. 4. The solid line represents the resulting flow curves, which were determined with the specimen made of deposition material. The dotted line represents the resulting flow curves of the specimen made of conventional material. First, both materials showed that the level of the flow stress k_f increases with increasing plastic strain until a plastic strain of 0.1 is reached. Subsequently the level of stress decreases. This behaviour is based on thermally activated recovery and recrystallization processes in the material at higher temperatures [11].

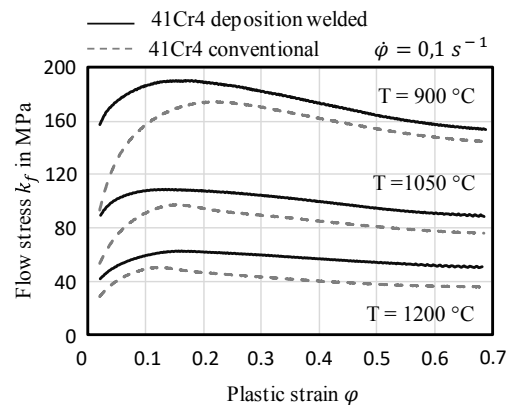


Fig. 4. Comparison of the flow behaviour of 41Cr4 between specimens made out of deposition welded and conventional material

In addition, the level of flow stress of the conventional and the deposition material differ. The level of the flow stress from deposition material is constantly higher than that of the conventional material. Also, the yielding point differ from each other at every investigated temperature. The deviation of the resulting flow curves is caused to different production methods of the specimen.

In Fig. 5 the resulting flow curves of X45CrSi9-3 of the deposition material at 900 °C, 1050 °C and 1200 °C at strain rate 1 s⁻¹ are presented (solid black lines). The solid grey lines represent comparative values from the simufact.forming database. In comparison to 41Cr4, the flow curves determined in the experiments only agree well with the database values under test conditions of 1200 °C. At 1050 °C and 900 °C, the level of flow stress of the welded material is significantly higher than the data of the simufact.forming database. In addition, the yielding point of the material is also about 200 MPa apart at 900 °C and at 1050 °C about 60 MPa. Also at 1200 °C the yielding point differs significantly. The results of the material characterisation indicate that the deposition-welded material has different properties than the values of the simufact.forming database or the data made by rod specimen made of conventional material. Therefore, it is necessary to carry out a material characterisation for each deposition-welded material separately.

In conclusion, the resulting flow curves of 41Cr4 of the deposition-welded material and the flow curves of the conventional material were similar. The parameters for the deposition welding process of X45CrSi9-3 should be investigated with the aim of approximating the flow behaviour of conventional material.

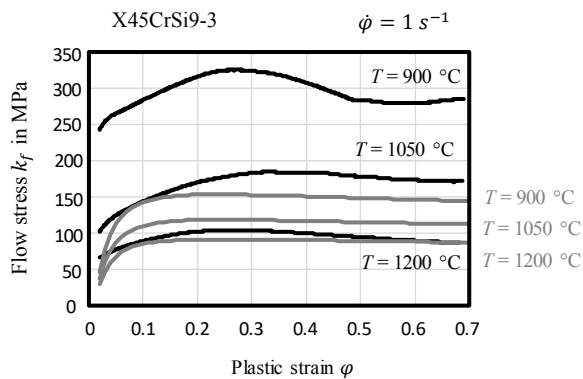


Fig. 5. Comparison of the flow behaviour of X45CrSi9-3 between specimens made out of deposition-welded and flow curves from the simufact database

4.2. Flow curve approach Hensel-Spittel-10

In this chapter, the results of the determination of the coefficients of the used Hensel-Spittel-10 are presented. The resulting stress-strain curves from the experimental tests were used to compute the required coefficients (cf. equation 1). To validate the coefficients of the Hensel-Spittel-10 flow curve approach, a numerical model of the uniaxial compression test was developed and the compression test was simulated. Subsequently, the resulting force-displacement curve from simulation and experimental tests are compared in Fig. 6. Three representative examples are presented there. The black solid

line shows the resulting force-displacement curve of the experimental setup and the dotted line the result of the numerical investigation. The tests were carried out at 900 °C and at strain rate 1 s⁻¹ with the material X45CrSi9-3. The light grey represents the results of conventional 41Cr4 at the test conditions of 900 °C and strain rate 0.1 s⁻¹. The last presented test was carried out at the test conditions 1200 °C and strain rate 0.1 s⁻¹. However, the deposition-welded material 41Cr4 was used. All three test conditions have in common that the resulting experimental and numerical force-displacement curves are in good agreement. This indicates that the Hensel-Spittel-10 approach used is suitable for mapping the flow behaviour of the material used. The computed coefficients are presented in Table 2.

Table 2. Computed coefficients for the used flow curve approach Hensel-Spittel-10 for the materials 41Cr4 conventional, 41Cr4 deposition and X45CrSi9-3 deposition

	41Cr4 conventional	41Cr4 deposition	X45CrSi9-3 deposition
A [Ns/mm ²]	467044	0.0189	0.0250
m ₁ [1/°C]	-0.0026	-0.0059	-0.0063
m ₂ [-]	0.1859	0.0385	0.2973
m ₃ [-]	-0.2563	0.0001	0.0010
m ₄ [-]	-0.0110	-0.0058	0.0049
m ₅ [1/°C]	-7.42 · 10 ⁻⁵	0.0012	0.0006
m ₆ [-]	-0.8706	-1.456	-1.3861
m ₇ [1/°C]	0.0003	0.0001	0.0001
m ₈ [-]	-0.7103	2.2025	2.3159

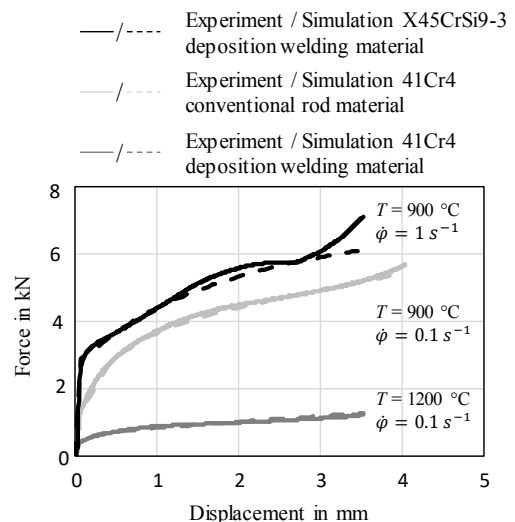


Fig. 6. Force-displacement curve of the uniaxial compression test

4.3. Numerical Results

In Fig. 7 (a) the bevel gear after the forming process is demonstrated, which was achieved with an initial inner layer thickness of 1 mm and an initial outer layer thickness of 3 mm. In the area of the formed tooth, only the materials of the welded layers are found. Fig. 7 (b) shows that the radial material flow

depends on the position in z-axis direction. In the lower area, the material is pressed strongly in the radial direction. The conical shape of the bevel gear and the selected conical shape of the bevel gear base caused this material distribution after the forming process. The strongest radial material flow occurs in the area of the burr.

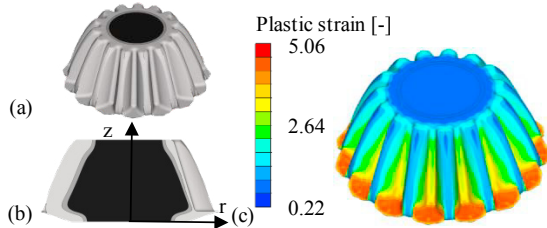


Fig. 7. (a) Bevel gear after the numerical simulation of the forming process, (b) section representation of (a), (c) plastic strain distribution that results after the numerical simulation of the forming process

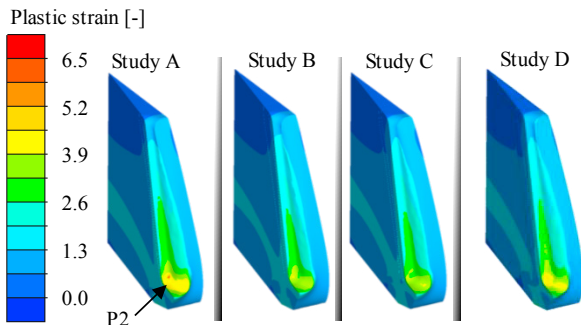


Fig. 8. Comparison of the plastic strain in the area of investigation point P2

The distribution of the plastic strain is shown in Fig. 7 (c). A degree of plastic strain of up to 5.06 is achieved in the area of the burr. In Fig. 9, the results of the numerical investigation with the initial layer thickness of the inner and outer layer according to Table 1 are presented. Fig. 9 shows a sectional view of the numerical results, which shall help to better pin the resulting material distribution in the tooth of the bevel gear after the forming process. The aim of the numerical investigation was the analysis of the material distribution after the forming process. Two points are used for the evaluation of the material flow. These points are named P1 and P2 and are marked in Fig. 9 section A and are the same in all following studies. P1 represents the point of force transfer at which high contact pressures arise and a sufficient layer of resistant material is required. In the area of point P2, the forming process results in strong material strain during the forming process. As a result, cracks of the material surface may occur. The thickness of the layer was measured in radial direction. The first result at section A of Fig. 9 represent the initial thickness of the inner layer with 1 mm and the outer layer with 1.5 mm. In the area of P2 the thickness of the inner layer is reduced to 0.39 mm and the outer layer to 0.17 mm. In this case, there could be cracks in the surface in the outer layer. These cracks are caused by high plastic strains. The distribution of the plastic

strain are presented in Fig. 8. In the case of study A the plastic strain is 6.5 in the area of investigation point P2 was achieved. This high plastic strain could cause cracks in the surface of the thin outer layer.

In the area of P1 a thickness of the outer layer of 0.76 mm and 0.92 mm of the inner layer is achieved. It is assumed that a sufficient layer thickness has been achieved in this area. This could also be determined in all other investigations and therefore in the following the results in the area of P2 will be discussed only.

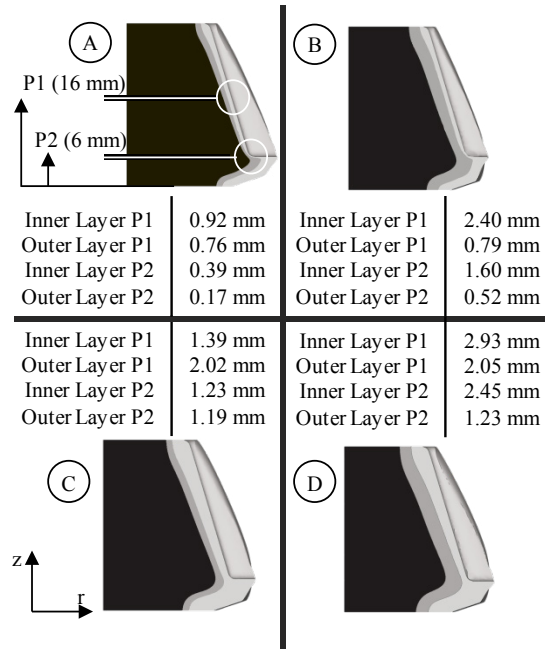


Fig. 9. Results of the numerical investigation, (A) initial inner thickness 1 mm outer layer 1.5 mm, (B) initial inner thickness 2 mm outer layer 1.5 mm, (C) initial inner thickness 1 mm outer layer 3 mm, (D) initial inner thickness 2 mm outer layer 1.5 mm

In study B, the thickness of the inner layer was increased from 1 mm to 2 mm. The outer layer was left at 1.5 mm. As in the first investigation, the thickness of the outer layer at P2 is reduced significantly to 0.52 mm. However, the plastic strain could be reduced by the supporting effect of the thicker inner layer to a value of about four (cf. Fig. 8).

Since the outer layer, like in study A, thins out considerably in this area as a result of the forming process the outer layer will be increase in the numerical studies B and C. The initial thickness of the inner layer was reduced to 1 mm and the outer layer was increased to 3 mm in study C. The results are presented in Fig. 9 in section C. Due to the higher initial thickness of the outer layer, the risk of cracks of the surface was reduced by a smaller thinning of the layer in the range of P2 (cf. Fig. 8). After the forming process, a layer thickness of 1.19 mm could be achieved in the area P2 of the outer layer.

In the last study D, the inner layer thickness was increased to 2 mm. The layer thickness of the outer layer kept constant at 3 mm. The resulting thicknesses in P2 for the outer layer were 1.23 mm and 2.45 mm for the inner layer, respectively. The increase of the initial layer thickness results in a supporting effect of the outer layer. This is reflected in a thicker outer layer

thickness after forming compared to the third test variant. The plastic strain in the outer stayed constant at about three.

In conclusion, the results of the numerical investigation show that there is a risk of cracks of the surface with an initial thickness of 1.5 mm of the outer layer in the area of P2. Due to an increase of the thickness of the outer layer, the high strains in the area of P2 could be reduced significantly.

5. Summary and Outlook

In this study, a material characterisation for deposition welded and conventional material was carried out to investigate the resulting flow behaviour by means of upsetting tests. The materials examined were 41Cr4 and X45CrSi9-3. The cylindrical specimens were extracted from welding tracks and from conventional rod material, respectively. Subsequently, the resulting flow curves were compared. The material characterisation showed that the flow behaviour of 41Cr4 of deposition welded material and conventional rod material are similar. However, level of flow stress of the deposition material is constantly higher than the conventional material. In contrast, the flow behaviour investigated for the steel grade X45CrSi9-3 differs significantly from the comparative values taken from the simufact.forming material database. The material characterisation outlined that the different manufacturing methods cause different material properties. In further research projects, the parameters of the welding process should be optimised in such a way that the flow properties of the welded material are approximated to the database values.

Furthermore, a numerical investigation of the forming process of a bevel gear was carried out. The aim of this investigation was to analyse the material distribution of the core and the two layer materials after the forming process. Four combinations of initial inner and outer layer thickness were investigated. In the investigated variants with an initial outer layer thickness of 1.5 mm, the layer thickness was thinned out during the forming process to such an extent that possible cracks could occur in the surface of the outer layer. By doubling the initial thickness of the outer layer to 3 mm, the thinning of the surface layer could be reduced. In further research, the resulting material distribution will be validated by means of experimental tests. In addition, the intermediate layer will be replaced with a material with a defined coefficient of thermal expansion. With this structure of the semi-finished product, specific residual stresses should be introduced into the bevel due to thermal tensions. These residual stresses should act against the loads that occur during the operating process. The aim of this design is to increase the service life in operation significantly. The lifetime studies are planned for the further course of the Collaborative Research Centre "Process chain to produce hybrid high-performance components".

Acknowledgements

The results presented in this paper were obtained within the Collaborative Research Centre 1153 "Process chain to produce hybrid high-performance components by Tailored Forming" in the subproject C1. The authors would like to thank the German Research Foundation (DFG / 252662854) for the financial and organisation support of this project. In addition, the authors would like to thank subproject A4 for the provision of semi-finished products for the material characterisation.

References

- [1] Goede M, Stehlin M, Rafflenbeul L, Kopp G, Beeh E. Super Light Car—lightweight construction thanks to a multi-material design and function integration. *Eur. Transp. Res. Rev.* 2009;1(1):5–10.
- [2] Behrens B-A, Overmeyer L, Barroi A, Frischkorn C, Hermsdorf J, Kaierle S et al. Basic study on the process combination of deposition welding and subsequent hot bulk forming. *Prod. Eng. Res. Devel.* 2013;7(6):585–91.
- [3] Kroner A. Hybrid forming is superior to joining technology. Düsseldorf.
- [4] Leiber R. ALUMINIUM: The ideal Material for hybrid forgings. Hannover Messe; 2011.
- [5] Politis D.J., Lin J., Dean T. Investigation of material flow in forging bi-metal components. *Steel Research International*; Available from: www.steelresearch-journal.com.
- [6] Kache H, Stonis M, Behrens B-A. Hybridschmieden: Monoprozessuales Umformen und Fügen metallischer Blech- und Massivelemente. *wt-online* 3-2013, Seite 257-262 2013, 2013.
- [7] Domblesky J, Kraft F, Druecke B, Sims B. Welded preforms for forging. *Journal of Materials Processing Technology* 2006;171(1):141–9.
- [8] Behrens B-A, Bouguecha A, Vucetic M, Huskic A, Uhe J, Frischkorn C et al. Umformtechnische Herstellung hybrider Lagerbuchsen. *wt Werkstattstechnik online* 2016;106:743–8.
- [9] Behrens B-A, Kosch K-G. Development of the heating and forming strategy in compound forging of hybrid steel-aluminum parts. *Mat.-wiss. u. Werkstofftech.* 2011;42(11):973–8.
- [10] Kaierle S, Barroi A, Noelke C, Hermsdorf J, Overmeyer L, Haferkamp H. Review on Laser Deposition Welding: From Micro to Macro. *Physics Procedia* 2012;39:336–45.
- [11] Pöhlandt K. Werkstoffprüfung für die Umformtechnik: Grundlagen, Prüfmethode, Anwendungen. Berlin, Heidelberg: Springer; 1986.
- [12] Weißbach. Werkstoffkunde. Springer Fachmedien Wiesbaden; 2015.
- [13] Henke T, Bambach M, Hirt G. Experimental Uncertainties affecting the Accuracy of Stress-Strain Equations by the Example of a Hensel-Spittel Approach. In: *AIP*; 2011, p. 71–76.
- [14] Behrens BA, Bouguecha A, Bonk C, Bonhage M, Chugreeva A, Matthias T. FE-Based Design of a Forging Tool System for a Hybrid Bevel Gear. *KEM* 2017;742:544–51.